**Biogeosciences
Discussions**

Stratigraphic analysis of lake level fluctuations in Lake Ohrid: an integration of high resolution hydro-acoustic data and sediment cores

K. Lindhorst[1], H. Vogel[2], S. Krastel[1], B. Wagner[2], A. Hilgers[3], A. Zander[3], T. Schwenk[4], M. Wessels[5], and G. Daut[6]

[1]Leibniz-Institute for Marine Sciences, IFM-GEOMAR, Cluster of Excellence: The Future Ocean, Christian-Albrecht-University, Kiel, Germany
[2]Institute for Geology and Mineralogy, University of Cologne, Cologne, Germany
[3]Institute of Geography, University of Cologne, Cologne, Germany
[4]Geoscience Department at University of Bremen, Bremen, Germany
[5]Institute for Lake Research, LUBW, Langenargen, Germany
[6]Institute for Geography, Friedrich Schiller University, Jena, Germany

Correspondence to: K. Lindhorst (klindhorst@ifm-geomar.de)

Stratigraphic analysis of lake level fluctuations in Lake Ohrid

K. Lindhorst et al.

Title Page

Abstract	Introduction
Conclusions	References
Tables	Figures

| ◄◄ | ►► |
| ◄ | ► |

Back | Close

Full Screen / Esc

Printer-friendly Version

Interactive Discussion

K. Lindhorst et al.

Abstract

Ancient Lake Ohrid is a steep sided, oligotrophic, karst lake of likely Pliocene age and often referred to as a hotspot of endemic biodiversity. This study aims on tracing significant lake level fluctuations at Lake Ohrid using high-resolution acoustic data in combination with lithological, geochemical, and chronological information from two sediment cores recovered from sub-aquatic terrace levels at ca. 32 and 55 m. According to our data, significant lake level fluctuations with prominent lowstands of ca. 60 and 35 m below the present water level occurred during MIS 6 and MIS 5, respectively. The effect of these lowstands on biodiversity in most coastal parts of the lake is negligible, due to only small changes in lake surface area, coastline, and habitat. In contrast, biodiversity in shallower areas was more severely affected due to disconnection of to-day sub-lacustrine springs from the main water body. Multichannel seismic data from deeper parts of the lake clearly imaged several clinoform structures stacked on top of each other. These stacked clinoforms indicate significantly lower lake levels prior to MIS 6 and a stepwise rise of water level with intermittent stillstands since its existence as water filled body, which might have caused enhanced expansion of endemic species within Lake Ohrid.

1 Introduction

Within the terrestrial realm, ancient lakes are valuable archives providing crucial information on past climate, environmental conditions, and speciation among endemic taxa. With its inferred existence since the Pliocene, its location in the northern Mediterranean borderland and its high degree of endemic diversity (Stankovic, 1960; Albrecht and Wilke, 2008), Lake Ohrid (Fig. 1) provides a unique site to study climatic and environmental changes over long time scales and their possible link to evolutionary patterns.

As documented by numerous paleoclimate studies, the Mediterranean region has experienced large scale climate fluctuations over the last glacial-interglacial cycle (e.g. Allen et al., 1999, 2002; Bar Matthews et al., 1999, 2000; Tzedakis et al., 2003; Martrat et al., 2004; Drysdale et al., 2005; Zanchetta et al., 2008; Vogel et al., 2010a).

5 While information on past temperature variability at relatively high spatial resolution has become available during the past decade (e.g. Peyron et al., 1998; Allen et al., 1999; Martrat et al., 2004; Hayes et al., 2005; Marino et al., 2009), information on hydrological changes in the northern Mediterranean borderland is relatively sparse over long time scales (Tzedakis et al., 2003; Bordon et al., 2009). In order to gain a better

10 understanding of the spatial variability of hydrologic changes in this climate sensitive region, additional spatially distributed paleoclimate records must be investigated. Ancient Lake Ohrid can provide such a record in the northern Mediterranean borderland with its sensitivity to recent and past climatic and environmental changes (Matzinger et al., 2006, 2007; Wagner et al., 2009; Vogel et al., 2010a). This promising loca-

15 tion, however, has never been the subject of a quantitative study reconstructing past changes in hydrology. The detection and dating of subaquatic and subaerial terraces is a robust approach to infer past variations in the hydrological budget of an individual lake (e.g. Magny et al., 2009; Moernaut et al., 2010).

Among different possible climate related factors affecting lacustrine ecosystems,

20 changes of the water budget and associated lake level fluctuations have been identified as one important mechanism influencing biodiversity (e.g. Johnson et al., 1996; Sturmbauer et al., 2001; Genner et al., 2010). This is because lake level fluctuations are commonly accompanied with changes of the lake chemistry, surface area, coastline, and habitat distribution and thus directly affect species living in the lake

25 (Martens 1997). Many studies have investigated lake level fluctuations (e.g. Scholz and Rosendahl, 1988; D'Agostino et al., 2002; Anselmetti et al., 2006; 2008; Daut et al., 2010, Moernaut et al., 2010) but in order to improve our knowledge on how lake level fluctuations influence biodiversity and speciation in lakes, uncertainties in magnitude and timing of lake level changes need to be quantified.

Seismo-acoustic data provide an image of continuous subsurfaces illustrating stacking trends, strata terminations, and geomorphology (Catuneanu et al., 2009). Depositional sequences can be subdivided into smaller stratigraphic units, termed system tracts, indicating their depositional regime during specific interval of relative lake level change (Posamentier et al., 1992, Hunt and Tucker, 1992, Allen and Allen, 2005). Shoreline trajectory describes the cross-sectional path of the shoreline as it migrates due to a change in lake level (Helland-Hansen and Martinsen, 1996). Three main factors determine the direction of the migration of the shoreline. These are the rate of relative lake level change, sediment supply, and basin physiography (Helland-Hansen and Martinsen, 1996). On a flat shelf area sediment is bypassed and falling relative lake level may cause the deposition of a set of downstepping prograding wedges in a forced regression system tract (FRST, Hunt and Tucker, 1992, Allen and Allen, 2005). Transgressive system tracts (TST) suggesting a rapid relative lake level rise often show an erosional surface (Allen and Allen, 2005). Following a rise in lake level a Highstand System Tract (HST) with clinoform geometries evolves that onlap onto the underlying sequence boundary in a landward direction (Allen and Allen, 2005). Clinoforms composed of topset, foreset and bottomset reflectors are the fundamental building blocks of sedimentary basins (Gilbert 1890, Pirmez et al., 1998).

While the magnitude of lake level change can be inferred relatively easily from the shoreline trajectory dating of one particular stillstand is a rather difficult task. Radiocarbon dating of organogenic macrofossils is one tool, which can provide age control for the past ca. 40 kyrs. Beyond that time, dating of lacustrine sediments requires other techniques with generally higher uncertainties. Positioned downwind of most of the Italian volcanoes active during the Quaternary, Lake Ohrid contains a sediment record that is an excellent archive of volcanic ash (Wagner et al., 2008a, b; Vogel et al., 2010b; Sulpizio et al., 2010). Since these tephra layers can be identified and, most importantly, correlated based on their chemical and morphological characteristics to eruptions with known ages, they serve as important stratigraphic and chronological markers. Other techniques such as luminescence and electron spin resonance (ESR) dating extend

the datable range of the lake terrace levels.

The main objectives of this study are to describe and quantify lake level changes within ancient Lake Ohrid that have been identified in seismic data up to a depth of 0.7 s Two Way Travel Time (TWT). We investigated patterns of lake level fluctuations by combining hydro-acoustic data with sedimentological and chronological data from lake sediment records. Specific objectives are: (i) to analyze whether lake level changes have occurred quickly, (ii) to date periods with constant lake levels in the past, (iii) to reconstruct ancient coastlines, (iv) to develop the paleoenvironmental evolution of Ohrid Bay since the penultimate glacial period (MIS 6) and finally (v) to evaluate whether changes of the lake surface area and volume can be linked to changes in biodiversity within ancient Lake Ohrid. Clinoforms observed in the southern area are used to infer the hydrological regime of Lake Ohrid prior to MIS 6 although direct correlations to ancient coastlines will only be possible with deep drilling cores.

2 Setting

Lake Ohrid (41°01′ N, 20°43′ E; Fig. 1) is located in a tectonically active graben system of the Western Macedonian geotectonic zone (Aliaj et al., 2001) at an altitude of 693 m.a.s.l. (Fig. 1). The lake has a maximum length of ca. 30 km, a maximum width of ca. 15 km, and covers an area of ca. 360 km^2 (Stankovic, 1960, Fig. 2). The morphology of the Lake Ohrid basin is relatively simple with a deep flat central basin, steep margins along major boundary faults at its eastern and western terminations, and shallow shelf areas in the northern and southern region (Wagner et al., 2008a, Fig. 2). The average water depth of the lake is ca. 150 m with a maximum water depth of 290 m and a total volume of 50.7 km^3 (Popovska and Bonacci, 2007, Fig. 2).

Karst aquifers, charged from precipitation on the surrounding mountain ranges and from its sister Lake Prespa, form up to 50% of the net inflow today (Matzinger et al., 2006, Fig. 2). Besides karstic inflows of the sublacustrine springs water enters Lake Ohrid by rivers and direct precipitation (Matzinger et al., 2006). Karstic springs can

be found at the present lake shore at three main locations, southwest of Struga, at the southern end of the lake basin, and in Ohrid Bay area (Popovska and Bonacchi, 2007, Fig. 2). At present, the Sateska and Cerava Rivers are the main riverine inflows to Lake Ohrid. Water leaves Lake Ohrid through the River Crn Drim (∼60%) and by
5 evaporation (∼40%, Matzinger et al., 2006, Fig. 2). No significant riverine inlets are found in close proximity to Ohrid Bay.

3 Methods

3.1 Hydro-acoustics

The first hydro-acoustic data were acquired in spring 2004 by means of a parametric
10 sediment echosounder (Wagner et al., 2008a). In September 2007 and June 2008 we carried out two multichannel seismic surveys using a small airgun (0.25 l and 0.1 l) and a 100 m-long 16-channel streamer. The processing procedure included trace editing, set-up geometry, static corrections, velocity analysis, normal move-out corrections, band-pass frequency filtering (frequency content: 35/60–600/900 Hz), stack, and time
15 migration. We applied a common midpoint spacing of 5 m throughout. During both multichannel surveys a parametric sediment echosounder with a main frequency of 10 kHz was operated simultaneously. Stacking of two adjacent pings improved the signal-to-noise ratio. We calculated water depth and penetration from the echosounder using a constant velocity of 1470 ms^{-1}. A dense net of sediment echosounder lines with a
20 spacing of less than 500 m (in Ohrid Bay even less than 100 m) has, through this study, become available for Lake Ohrid (Fig. 2).

Sidescan sonar data were acquired in 2008 using a Klein 3000 dual frequency sonar with 100 kHz and 500 kHz. The Ohrid Bay area was mapped between 3 and about 100 m water depth. The sonar was usually adjusted to cover 75–100 m on either side
25 with individual profiles spaced 75–100 m apart. In this way, complete coverage for the mapping area was achieved.

In September/October 2009, we collected high-resolution bathymetric data by means of ELAC Seabeam 1180 system. The system uses 126 beams with a total opening angle of 153° and operates with a frequency of 180 kHz. The transducers were mounted at the bow of the vessel. Vessel motion was measured using an OCTANS IV motion sensor that provides roll, pitch, and heave correction. We collected sound velocity profiles at different locations across Lake Ohrid. Processing of the data was mainly done by means of the software package MBSystem and GMT (Wessel and Smith, 1991, Caress and Chayes 2005). The area of Ohrid Bay is covered from 20 m water depth into deep basin.

3.2 Sediment cores

Cores Co1200 and Co1201 were recovered in fall 2007 from the northeastern part of Lake Ohrid where hydro-acoustic surveys indicated two sub-aquatic terrace levels at 32 and 55 m water depth (Fig. 3). The surface sediments and deeper sediments were collected using a 0.6-m gravity corer and a 3-m-long percussion piston corer, respectively (both UWITEC Co). The overlapping 3-m long core segments were subdivided into 1-m-long segments in the field.

Prior to sub-sampling one core halve was used for high-resolution X-ray fluorescence (XRF) scanning by means of an ITRAX core scanner (COX Ltd.), equipped with a Mo-tube set to 30 kV and 30 mA and a Si-drift chamber detector. Scanning was performed at 2.5 mm resolution and an analysis time of 20 s per measurement. The obtained count rates for Ti, K, and Ca can be used as estimates of the relative concentrations for these elements (Croudace et al., 2006).

Sub-sampling was performed at 2 cm intervals. The water content (WC) for each sample was determined from the weight difference between wet and freeze-dried samples. Aliquots of the freeze-dried subsamples were ground to a particle size below 63μm using a planetary mill for subsequent biogeochemical analyses, which was done at 6 cm resolution. Total carbon (TC) concentrations, were measured with a Vario Micro Cube combustion CNS elemental analyzer (VARIO Co). Samples for total organic

carbon (TOC) analysis were pre-treated with HCl (10%) at a temperature of 80°C to remove carbonates and then analyzed using a Leco CS-225 carbon-sulfur detector (LECO Corp.). The amount of total inorganic carbon (TIC) was determined from the difference between TC and TOca. The calcite ($CaCO_3$) content was calculated from
5 TIC under the assumption that TIC solely originates from $CaCO_3$.

In order to develop a chronological framework for cores Co1200 and Co1201 radiocarbon, infrared stimulated luminescence (IRSL), electron spin resonance (ESR) dating, and tephrostratigraphy was applied. For radiocarbon dating plant macrofossils from 6 and 13 cm depth in core Co1200 and from 15 and 18 cm depth in core
10 Co1201 were used (Table 1). Radiocarbon dating was performed by accelerator mass spectrometry (AMS) at the Leibniz Laboratory for Radiometric Dating and Isotope Research in Kiel, Germany. The obtained ages were calibrated into calendar years before present (cal. yr BP) using CalPal-2007 online and the CalPal2007_HULU calibration curve (Danzeglocke et al., 2008).
15 IRSL dating was solely performed on four samples from core Co1201. In the laboratory under subdued illumination about 20 cm^3 material was taken from four different depths (340–377, 377–408, 503–550, and 550–597 cm; Table 2) using the core half, which was not XRF scanned. Additionally samples at each of the four depths were taken for dose rate measurements. The concentrations of U, Th and K were deter-
20 mined by gamma-ray spectrometry using approximately 400 g of sediment per sample. Several dating attempts applied to quartz extracts like a standard optically stimulated luminescence single aliquot regeneration protocol or an isothermal TL approach failed due to saturation effects. Hence, IRSL measurements were carried out on potassium-rich feldspar extracts in the blue detection range (410 nm interference filter) using a
25 single aliquot regeneration protocol. Fading tests and fading corrections were applied to the IRSL ages as described by Auclair et al., (2003) and Lamothe et al., (2003, see also Preusser et al., 2008 for further details on luminescence dating and the problem of fading).

Stratigraphic analysis of lake level fluctuations in Lake Ohrid

K. Lindhorst et al.

We performed ESR dating only on one horizon in core Co1200 (Table 2). For this purpose we collected large mollusk shell fragments from a horizon at 230–262 cm depth. In order to determine the radionuclide contents of the surrounding sediment and of the mollusks themselves ICP-mass spectrometry were applied. We carried out ESR
5 measurements using an additive dose protocol for multiple aliquots (Schellmann et al., 2008).

Both cores Co1200 and Co1201 contained peculiar horizons consisting almost entirely of volcanic glass shards (tephra). Tephra horizons in core Co1200 occur at 38–40 (OT0700-1) and 85.5–120.5 (OT0700-2) cm. Tephra horizons in core Co1201 occur
10 at 110–126 (OT0701-5), 184–186 (OT0701-6), and 190–192 (OT0701-7) cm. From these horizons we washed and sieved about 1 cm^3. The >40µm fraction was embedded in epoxy resin and screened for glass shards and micro-pumice fragments using scanning electron microscopy (SEM). We performed energy-dispersive-spectrometry (EDS) analyses of glass shards and micro-pumice fragments using an EDAX-DX
15 micro-analyzer mounted on a Philips SEM 515 (operating conditions: 20 kV acceleration voltage, 100 s live time counting, 200–500 nm beam diameter, 2,100-2,400 shots per second, ZAF correction).

4 Results

4.1 Ohrid Bay

20 #### 4.1.1 Bathymetry and lake floor morphology

High-resolution bathymetric data gathered offshore from the City of Ohrid is characterized by three distinct morphological steps divided by areas of gently dipping (<1°) plateaus (upper and lower terraces, Fig. 3). The terminology used for each data set within Ohrid Bay is summarized in Table 3. After a first terrace in 15 m profiles run-
25 ning in an east-west direction show a second drop in topography at a water depth of

about 30 m. The outer edge of this second terrace is characterized by a sharp break in the slope gradient from ~2° to ~4°, which can be traced in a half circle parallel to the present-day northern coastline. At a depth of ~55 m another prominent step in topography is observable (Fig. 3). At this step the lake floor drops to more than 200 m water depth with a slope angle of up to 10° down into the central basin. A sub-lacustrine basement high that crops out in the southern part of the Ohrid Bay area is clearly visible in the high-resolution bathymetric data (Fig. 3).

A side scan sonar mosaic images the surface texture of each individual terrace. High backscatter values along morphological steps mark exposures of terrace-building sediment sequences (Fig. 3). Small-scale patches of strong backscatter values on top of the upper terrace in a water depth of 30 m are indications of ancient eroded surfaces partly overlain by younger sediments. The distribution of macrophytes in littoral areas of Ohrid Bay is traceable by side scan sonar data.

4.1.2 Stratigraphy

The sediment echosounder dataset covers the entire Ohrid Bay showing the internal structure of the sediments up to a depth of 50 m below the lake bottom. The net of seismic lines is very densely spaced (Fig. 4, map inlet). A set of parallel lines is running from north to south with a line spacing of less than 100 m. In addition, numerous profiles were collected from the central lake basin perpendicular to the coastline across both terraces. The density of high-resolution seismic profiles allows us to correlate between the profiles.

Stratigraphic Unit E is divided into sub-units E1 and E2 (Fig. 4). Sub-unit E1 is characterized by oblique, parallel to sub-parallel reflectors with increasing dip angles to the west, and a toplap as upper boundary. Due to the limited penetration of the acoustic waves, the lower boundary of Sub-unit E1 and hence the basin physiography cannot be detected. A steep slope with an angle of 15° forms the transition to the profundal part of the lake. Sub-unit E2 a prograding clinoform with medium amplitude reflections (Fig. 4) is stacked on top of sub-unit E1.

Full Screen / Esc

Printer-friendly Version

Interactive Discussion

Unit F appears in the seismic data as a low-amplitude wedge truncated by erosional surfaces on top and to the west. Penetration into Unit F is limited, therefore only a few internal reflections are visible that indicate slightly dipping strata (Fig. 4). Towards the west, Unit F crops out and causes high backscatter visible in the sidescan data.

Sediment depositions assigned to units G and H are found on both terraces. In a water depth of about 50 m (lower terrace) Unit G onlaps onto Unit F suggesting a transgressive sequence boundary (Fig. 4). A thinning of strata towards the west is observed. In close proximity to the lakeshore at water depths of about 30 m (upper terrace), sediments of units G and H discordantly cover Unit F. A prominent horizon within Unit G can be assigned to Y-5 tephra (see below). The youngest seismic Unit H is recognized by slightly lower-amplitude reflections. A hummocky topography on both terraces indicates deposits of mass wasting processes (Fig. 4).

The cores recovered from the terraces in Ohrid Bay, measured after correlation of individual segments using XRF data and lithological core descriptions 2.63 m (Co1200) and 5.97 m (Co1201). Lithological characteristics, geochemical indicators, and chronological constrains imply a subdivision of the sedimentary successions of cores Co1200 and Co1201 into four distinctly different lithological facies (Figs. 5 and 6).

Lithofacies IV forms the basal succession of core Co1201 between 597 and 305 cm depth and is limited at its top by a 0.5 cm thick sand layer with clear erosional base (Fig. 6). The sediments appear laminated with laminae width of 0.2–1 cm, dark to light grey, and are mainly composed of clastic sandy silt. The dominance of clastic material in Lithofacies IV is well correlated to high Ti and K intensities. Terrestrial plant macrofossils and reworked mollusk shells are abundant in variable quantities explaining relatively high TOC concentrations and detectable amounts of $CaCO_3$. Chronological control for Lithofacies IV sediments is given by IRSL dating of feldspar specimens sieved from the sand fraction of four horizons. IRSL dating on feldspars from the horizons at 340–377, 377–408, 503–550, and 550–597 cm yielded ages of 157 ± 21, 181 ± 24, 123 ± 16, and 143 ± 21 ka, respectively (Fig. 2). These results can be regarded as minimum ages, since underestimation of the burial age for feldspar samples from deposits

beyond 100 ka notwithstanding correction procedures can be assumed (Wallinga et al., 2007). Dose rate measurements yielded very consistent nuclide concentrations (Table 2) for the four samples, suggesting a uniform sediment deposition. By contrast, the IRSL ages show no age increase with depth but an inconsistent array. This indicates partly insufficient bleaching before deposition or to post-sedimentary influences and changes in the stratigraphic sequence after sedimentation. Variations in density, thickness of the overlying sediments or the water column do affect the dose rate calculations and might also contribute to the scatter of the ages. Taking all uncertainties into account, the IRSL dating results support a correlation of this stratigraphic unit with MIS 6.

Lithofacies III comprises the basal succession of core Co1200 between 263 and 181.5 cm (Fig. 5). A similar lithofacies is absent in core Co1201 (Fig. 6). Sediments assigned to Lithofacies III appear grayish-white and consist almost entirely of silt-sized authigenic calcite ($CaCO_3 > 70\%$) and mollusk shells of their fragments. As indicated by extremely low Ti and K intensities clastic matter is almost absent. Low TOC ($< 1.2\%$) concentrations originate from finely dispersed organic matter (OM) and few leave and shaft fragments of chara algae. ESR dating of mollusk shells collected in between 262 and 230 cm yielded a modeled age of 130 ± 28 ka (Table 2). This age, however, has a high uncertainty, because the post-depositional history regarding the thickness of the overlying sediment and water column has a high impact on the dose rate calculation for these deposits with very low radioactivity. A larger data set would be preferable to support this first estimation. The transition from sediments of lithofacies III to II in core Co1200 is abrupt and occurs within a few centimeters. These transitional centimeters contain gravel, sand, and reworked mollusk shells without any grading.

Sediments deposited between 181.5–120.5 and 85.5–16 cm in core Co1200 (Fig. 5) and between 305–126 and 110–18.5 cm in core Co1201 (Fig. 6) are assigned to Lithofacies II. Its sediments appear dark-gray and consist of clastic clayey-sandy silts with frequent occurrences of gravel grains. Small reworked shell fragments occur in low abundance at both sites. $CaCO_3$ concentrations are $<40\%$ and TOC concentrations

Title Page

Abstract | Introduction

Conclusions | References

Tables | Figures

◄ | ►

◄ | ►

Back | Close

Full Screen / Esc

Printer-friendly Version

Interactive Discussion

are <2%. Despite the general similarities for Lithofacies II sediments at both sites, some differences were also observed. For example, larger intact chara fragments are abundant in sediments of core Co1200, but only small leave and shaft pieces were found in core Co1201. Another difference is the amount of finely dispersed OM and CaCO$_3$, which is higher in Lithofacies II of core Co1200 compared to Co1201. A prominent and extensive tephra horizon occurs between 120.5–85.5 cm in core Co1200 and 126–110 cm in core Co1201. Geochemical and morphological correlation of glass shards from both tephra deposits point to the Campanian Ignimbrite (CI)/Y-5 eruption of the Campi Flegrei Caldera (Sulpizio et al., 2010), which is Ar/Ar dated to 39.2 ± 0.1 ka (De Vivo et al., 2001). Apart from this extensive tephra deposit found in both cores (Figs. 5 and 6) additional tephra layers were recognized in core Co1200 at 40–38 cm (OT0700-1), in core Co1201 at 186–184 cm (OT0701-6), and 192–190 cm (OT0701-7). Tephra OT0700-1 was successfully correlated to the Y-3 tephra layer (Sulpizio et al., 2010), which is dated at 30.67 ± 0.2 ka (Sulpizio et al., 2003). Tephra layer OT0701-6 correlates to the C20/ SA3-b tephra layer (Sulpizio et al., 2010) dated at 79–80 ka (Paterne et al., 1988). The OT0701-7 tephra layer likely corresponds to the TAU1-b/X-5 tephra layer (Sulpizio et al., 2010), which has an age of 105 ± 2 ka (Keller et al., 1978; Kraml, 1997).

The transition from Lithofacies II to Lithofacies I is characterized by a 2–3 cm thick sand layer between 16–13 cm (Co1200, Fig. 5) and 18.5–16.5 cm (Co1201, Fig. 6) with apparent erosive base in both cores. The sand layers show no upward fining in grain size, which would be typical for deposition from turbidity current, but is probably best explained as originating from some sort of mass movement process rather than lake level low stand. Radiocarbon dating of plant macrofossils just below the sand layer at 13 cm in core Co1200 and at 18 cm in core Co1201 yielded ages of 25815 ± 522 and 19030 ± 244 cal. yr BP (Table 1), respectively, implying a hiatus in the cores after the Last Glacial Maximum (LGM).

Lithofacies I occurring in both cores (0–13 cm in Co1200 and 0–16.5 cm in Co1201; Figs. 5 and 6) as light-brown layer is composed of calcareous (CaCO$_3$ > 40%) clayey

silt and contains complete bivalve shell and their fragments. TOC concentrations of up to 2% can be explained by finely dispersed organic matter (OM) as well as small leave and shaft parts from chara algae. Radiocarbon dating of plant macrofossils from Lithofacies I at 15 cm in core Co1201 yielded an age of 5773 ± 82 cal. yr BP (Table 1).

5 The modern age of plant macrofossils from 6 cm in core Co1200 is probably a result of contamination with recent plant material.

4.2 Southern area

We observed several well-preserved prograding delta deposits within multichannel seismic data in the southern part of Lake Ohrid reflect significant lake level changes in

10 the past (Fig. 7). Stacked sigmoidally shaped clinoforms are recognized in the seismic cross section (Fig. 7). These clinoforms are characterized by low-amplitude bodies composed of topset, foreset, and bottomset reflectors. Reflections within individual clinoform packages are marked in the interpreted seismic section in Fig. 7. Several high-amplitude reflectors overlie each wedge and are numbered as 1 to 5 from oldest

15 to youngest.

Further basin-ward from the clinoforms seven depositional sequences (A to G) were defined by tracing unconformities or their correlative conformities of reflectors bounding clinoform structures. The acoustic basement that limits penetration is recognized in the southern part of the profile rising up from the deeper central basin towards shallower

20 shore areas. Unit A, the oldest sequence overlying the basement is characterized by several high amplitude reflectors. Units B and C have very similar seismic characteristics showing well-stratified, continuous reflectors with medium amplitudes that onlap on foresets of clinoforms. Within each unit one or more prominent reflectors are observed and marked in the interpreted section (Fig. 7). The next younger units, D

25 and E, display the most complex seismic architecture within this cross-section. Three major mass movements deposits (S2 to S4, Fig. 7), defined by transparent units, are identified in units D and E. Prominent and continuous horizons occasionally mark the base of such failure events and divide the unit in sub-units. Additional high-amplitude

reflectors within Unit E are well imaged. We speculate that the top of Unit E most likely marks the transition of the penultimate glacial period (MIS 6) to the last interglacial period (MIS 5) as the bounding reflector is of the same age as its counterpart in Ohrid Bay. Furthermore, units F and G correspond to the last interglacial period (MIS 5),
5 and the last glacial period (MIS 4, 3, 2), respectively. Although a direct correlation to cores in Ohrid Bay is not possible, prominent reflectors of each individual unit (F and G) can be traced to a core located within the bottomset of the lower terrace assigned to Lithofacies IV (Vogel et al., 2010b) and therefore are reliably dated to the same age as their corresponding units identified in Ohrid Bay. Within well-stratified sediments of
10 Unit G, a prominent reflector most likely correlates to tephra layer Y-5 found in both cores described in this study (Figs. 4–7) as well as in Co1202 (Vogel et al., 2010a, b). Towards the north, one thick slide deposit characterized by a chaotic seismic facies are onlapping on well-stratified sediments of Unit G. Seismic stratigraphic units described above can be traced into the central basin characterized by thick undisturbed
15 sediments (Fig. 7c).

5 Discussion

5.1 Paleoenvironmental reconstructions

Based on the data available, we reconstructed four main phases of lake level dynamics back to MIS 6 in Ohrid Bay. In a temporal context these phases can be described as
20 followed: (1) the buildup of a lower terrace, 55 m below the present water table (Unit E1, Lithofacies IV) during the penultimate glacial period (MIS 6), (2) the development of the upper terrace (Unit F, Lithofacies III) during the last interglacial period (MIS 5), (3) sedimentation of Lithofacies II assigned to seismic Unit G during the last glacial period, and (4) mid-Holocene to modern sedimentation as evident by Lithofacies I
25 referring to seismic Unit H.

Coarse silt to sand-sized clastic material, which dominates Lithofacies IV, along with relatively large and in combination of the width of the lower terrace, implies sedimentation close to a river mouth over a significant time span. The seismic and sedimentological data suggest that the water-level of Lake Ohrid was up to 55 m lower than today, which could be due to significantly drier conditions. A drier climate at Lake Ohrid during MIS 6 correlates well with other reconstructions from northeastern Greece (Tzedakis et al., 2003) and the Levant region (Bar Matthews et al., 2003) and infers that most of the eastern Mediterranean was affected by these conditions. Since there is no significant inlet close to Ohrid Bay today, we assume that dewatering of the watershed during MIS 6 differed significantly in the past.

The only significant valley, which enters the Ohrid Bay, is a valley expanding from the northwestern slope of Galicica Mountains (Fig. 2). Today, this valley is not drained by a significant river. However, higher discharge in the past, with a significant supply of clastic material forming the lower terrace, could have been due to abundance and advance of local glaciers, which are known to have reached mid-valley positions during MIS 6 in the region (Hughes et al., 2006). Even though climate conditions were probably significantly drier than today these glaciers might have supplied enough water and eroded material during spring - summer melt water pulses.

The observed sediment characteristics of Lithofacies III deposited on the upper terrace (Table 1), in combination with chronological and stratigraphical constrains, point to deposition of the corresponding sediments in a shallow-water, low-energy regime during the last interglacial period. The identification of gently dipping foresets supports a deposition of material in low-energy regime. Wave-action, however, transported material towards the edge of the sub-aquatic terrace. Input of coarse-grained clastic material by riverine inflows was negligible, thus implying the river draining the valley on the northeastern slope of Lake Ohrid has not been active during the last interglacial period (MIS 5). The observed sediment characteristics and location of the upper terrace indicate warm and dry climate conditions during its formation. Although warm climate conditions during the last interglacial period are reported from to other paleoclimate

records (Tzedakis et al., 2003; Martrat et al., 2004; Allen and Huntley 2009; Vogel et al., 2010a), drier climate conditions seem to be restricted to the Ohrid area.

The sediment composition of Lithofacies II, the CI/Y-5 tephra, radiocarbon ages further up-core, widely intact chara specimen, and significant amounts of $CaCO_3$ and TOC in site Co1200 suggest that this facies was deposited at 3–20 m water depth within the littoral chara belt, when the water level during the last glacial period was lower than today. A cliff-like feature observed within Unit F and onlapping reflectors of units G and H are evident in the seismic data and imply that the upper terrace has been exposed after its initial formation (Fig. 4).

The most recent sediments comprising Lithofacies I in cores Co1200 and Co1201 represent a deposition of mid-Holocene to modern-day sediments at both sites. Since larger intact chara fragments and coarser clasts are absent throughout Lithofacies I we conclude that both sites remained well below the chara belt (>30 m) throughout the period of deposition. The hemipelagic characteristics of units G and H suggest environmental conditions comparable to those of today.

5.2 Lake level fluctuations and biodiversity

We interpreted four major shoreline trajectories since the penultimate glacial period as inferred from sediment echosounder data from Ohrid Bay, which were combined with lithological information (Fig. 8). These steps include: (i) a forced regression system tract (FRST 6), (ii) a Highstand System tract (HST 7), (iii) a minor FRST 8, and finally (iv) a transgressive system tract or HST 9. All numbers referring to lake levels are given in meters below the modern water table.

A base level for the formation of FRST 6 (Fig. 8a) cannot clearly be identified. However, ostracods found within cores taken on land in vicinity to Ohrid Bay suggest that the shoreline of the lake was further landwards than present (Hoffmann et al., 2010). Hence we conclude that the base level must have been higher than today. A maximum of regression at a base level of 55 m is evident by truncation of topsets of FRST 6 (stage 1, Fig. 8b). A relative lower terrace still evident within the modern morphology

further suggests that the process of sediment bypassing took place over a long period (Figs. 3, 4, 8).

HST 7, which is only detectable by sediment echosounder data (Figs. 4, 8) and stacked on top of FRST 6, probably formed after a subsequent transgression to a base level of about 25 m (stage 2, Fig. 8b). Since the sediment cores did not recover material from sub-unit E_2, exact dating of this period was not possible. Based on the deposition of HST 7 on top of the truncated surface of FRST 6, we suggest that HST 7 occurred during late MIS 6 or early MIS 5 (Fig. 8b).

A minor drop within MIS 5 (stage 3, Fig. 8c) following the previous HST 7 period is evidenced by FRST 8 (Unit F and Lithofacies III). Since Unit F shows evidences for calm conditions during deposition and subsequent sub-aerial exposure we conclude that the base level fell below the upper terrace level to a depth of about 35 m (Fig. 8c).

Finally, seismic units G and H as well as lithofacies II and I point to a rapid lake level rise and subsequent stillstand after FRST 8, which led to depositional conditions of hemipelagic sediments that is still ongoing today (Fig. 8d).

The effect on the coastlines for the significant lake level fluctuations since the penulti-mate glacial period is illustrated in Figure 9. Reconstruction of these ancient coastlines shows that only relatively small areas are affected by a 60 m drop in lake level. How-ever, these areas are important for the endemism in Lake Ohrid (Albrecht and Wilke, 2008). For example, the area close to Veli Dab, the feeder springs near Sveti Naum, and its sister complex Tushemisht/Zagorican are areas showing indications for punctual endemism and are located within the uppermost 60 m of the lake (Fig. 9, Albrecht and Wilke, 2008). Furthermore, Hauffe et al. (2010) observed that almost all gastropods live within a depth zone of 5–50 m. A minor drop in lake level may lead to a disconnection and/or isolation of certain areas from the proper lake resulting in allopatric speciation. Therefore we suggest that the evolution of endemic species is tentatively correlated with significant lake level fluctuations. Nevertheless this correlation remains specu-lative due to high uncertainties in speciation rate (Martens, 1997) and the timings of lake level stages or changes (Genner et al., 2010 and this study). Allopatric speciation

Stratigraphic analysis of lake level fluctuations in Lake Ohrid

K. Lindhorst et al.

involves a strict geographical barrier that prevents or reduces gene flow among sub-populations (for details see Albrecht and Wilke, 2008), and such a barrier apparently did not exist in ancient Lake Ohrid. The bathymetry of Lake Ohrid indicates that no sub-basins or sub-aerial islands existed during MIS 6, when the base level was 60 m lower than present day (Fig. 8). In comparison to the African Lake Malawi, where a magnitude of lake level changes greater than 550 m and subsequent expansion and establishment of rock fish populations was reconstructed (Genner et al., 2010), the magnitude of lake level change for Lake Ohrid since MIS 6 was probably too small for a major effect on speciation. One explanation is that the inferred lake level changes at Lake Ohrid had only a minor impact on the environment, particularly at the eastern shore, where rocky cliffs continue into deeper waters and an adaptation of species to a new living environment was not necessary. A change from calm conditions during lake level highstands to more dynamic conditions within the littoral zone after a drop in lake level may have an effect on species, which have been evolved during calm conditions as explained by Martens (1997). Within Lake Ohrid this is valid for small areas bounded by cliffs along the eastern shore line and more importantly within Ohrid Bay. These areas, although they were not completely desiccated, experienced a significant change in water depth with subsequent change in dynamic conditions.

Significant changes could have also affected the northern shore area where the bathymetry indicates a gently dipping sandy lake floor (Fig. 9). Here, even a minor transgression/regression of the shoreline would lead to drastic changes of subsurface properties and, subsequently, may have a major impact on the living environment.

In a longer term perspective, the endemism in the lake could have been affected by gradual lake level rise, when Lake Ohrid became established as water filled body. This lake level rise can be deduced from the five clinoform structures seen in the multichannel seismic data (Fig. 7) at the southern part of Lake Ohrid. Ancient depths of lake levels can be estimated by picking topset reflectors. Using an average sound velocity of 1600 m/s for sediments, distinct reflectors occur at 200, 285, 300, 330, and 360 m depth below the modern lake level. We cannot assume that these numbers

K. Lindhorst et al.

directly correspond to ancient lake levels because the subsidence history of the basin is not well known and current depths of the clinoforms are a combined effect of tectonic movements and lake level fluctuations. Nevertheless, pronounced clinoforms indicate significantly lower lake levels in the past with subsequent sudden changes in lake level.

5   A first attempt of dating individual clinoforms was done by tracing reflectors directly above or below the clinoforms to areas of undisturbed sediments within the central lake basin and assuming constant sedimentation rates. For example, the reflection interpreted to mark the transition of MIS 6 to MIS 5 can be traced all over Lake Ohrid. By using this reflector as a marker horizon an average sedimentation rate of 0.28 mm/yr

10   for the period younger than 130 ka can be calculated for the deep basin. This sedimentation rate would provide an age of ca. 41 ka for the Y-5 tephra, which is close to its real age. Extrapolation of this sedimentation rate leads to age estimations of ∼510, ∼600, ∼800, ∼940, and ∼1100 ka for the base of Unit E, D, C, B, and the basement (or base of Unit A), respectively. However, these numbers are only first estimates and

15   inhibit great uncertainties due to a lack of lithological information of sediments older than 130 ka. For example, our age estimate for the basement is much lower than ages suggested by other authors (Aliaj et al., 2001; Spirkovski et al., 2001; Dumurdzanov et al., 2005; Susnik et al., 2006) though the actual age of Lake Ohrid is still highly debated. The calculated ages can probably regarded as minimum values as velocities

20   for sediments increase with depth and our model does not include possible hiatuses that would lead to older ages for the basement of Lake Ohrid. Seismic stratigraphy, however, shows that clinoforms offshore Sveti Naum are significantly older than MIS 6 (Fig. 7). Final interpretation can only be achieved by combining seismic data with the information from a deep drilling campaign, which will provide crucial information for

25   reconstructing the subsidence history of the basin and a profound age model for the older sediments.

6 Conclusions

Our study illustrates that a combined geophysical and sedimentological approach is a powerful tool to investigate lake level fluctuations and link them to biodiversity in ancient lakes. Hydro-acoustic data show that Lake Ohrid has undergone significant lake level fluctuations. Multichannel seismic data penetrating into deeper parts of sediments suggest that, in general, lake level rose stepwise since its establishment as water filled body. The topset reflections up to depths of 360 m below modern lake level as evident by pronounced clinoforms offshore Sveti Naum suggest that the surface area of Lake Ohrid was significantly reduced in former times. Further lithological data is needed to reduce uncertainties with respect to age estimates of prominent reflections as well as the subsidence history of the entire basin. An analysis of sediment echosounder profiles and core data within Ohrid Bay allows a more detailed reconstruction back to the penultimate glacial period. Two terraces are well preserved as morphological pattern within Ohrid Bay. The lower terrace (Unit E1, Lithofacies IV, FRST 6) is most likely a relict of a fan delta that formed in a high energy shallow water environment close to a river mouth during MIS 6. In contrast, the upper terrace (Unit F, Lithofacies III, FRST 8) formed in a low energy regime potentially under warm climate conditions with only minor rivers draining into Ohrid Bay during MIS 5. Four major shoreline trajectories can be deduced since the penultimate glacial period. A formation of sub-basins or sub-aerial parts since penultimate glacial is unlikely, since the lake level lowering by 30 or 60 m did not significantly affect the overall surface area of Lake Ohrid. However, the lake level changes may have had a significant impact on the speciation, since a great proportion of endemic species are found above 50 m water depth in modern Lake Ohrid.

References

10 Albrecht, C. and Wilke, T.: Ancient Lake Ohrid: biodiversity and evolution, Hydrobiologia, 615, 103–140, 2008.

Aliaj, S., Baldassarre, G., and Shkupi, D.: Quaternary subsidence zones in Albania: some case studies, B. Eng. Geol. Environ., 59, 313–318, 2001.

Allen, J., Brandt, U., Brauer, A., Hubberten, H., Huntley, B., Keller, J., Kraml, M., Mackensen, A.,
15 Mingram, J., and Negendank, J.: Rapid environmental changes in southern Europe during the last glacial period, Nature, 400, 740–743, 1999.

Allen, J., Watts, W., McGee, E., and Huntley, B.: Holocene environmental variability - the record from Lago Grande di Monticchio, Italy, Quatern. Int., 88, 69–80, 2002.

Allen, P. A. and Allen, J. R.: Basin Analysis Principes and Applications, 2 Edn., Blackwell
20 Publishing, 2005.

Anselmetti, F., Ariztegui, D., Hodell, D., Hillesheim, M., Brenner, M., Gilli, A., McKenzie, J., and Mueller, A.: Late Quaternary climate-induced lake level variations in Lake Petén Itzá, Guatemala, inferred from seismic stratigraphic analysis, Palaeogeogr. Palaeocl., 230, 52–69, 2006.

25 Anselmetti, F., Ariztegui, D., Batist, M., Gebhardt, A., Haberzettl, T., Niessen, F., Ohlendorf, C., and Zolitschka, B.: Environmental history of southern Patagonia unravelled by the seismic stratigraphy of Laguna Potrok Aike, Sedimentology, 2008.

Auclair, M., Lamothe, M., and Huot, S.: Measurement of anomalous fading for feldspar IRSL using SAR, Radiation measurements, 37, 487–492, 2003.

30 Bar-Matthews, M., Ayalon, A., Kaufman, A., and Wasserburg, G.: The Eastern Mediterranean

Stratigraphic analysis of lake level fluctuations in Lake Ohrid

K. Lindhorst et al.

Title Page

Abstract	Introduction
Conclusions	References
Tables	Figures

Back | Close

Full Screen / Esc

Printer-friendly Version

Interactive Discussion

paleoclimate as a reflection of regional events: Soreq cave, Israel, Earth Planet. Sc. Lett., 166, 85–95, 1999.

Bar-Matthews, M., Ayalon, A., and Kaufman, A.: Timing and hydrological conditions of Sapropel events in the Eastern Mediterranean, as evident from speleothems, Soreq cave, Israel, Chem. Geol., 169, 145–156, 2000.

Bar-Matthews, M., Ayalon, A., Gilmour, M., Matthews, A., and Hawkesworth, C.: Sea-land oxygen isotopic relationships from planktonic foraminifera and speleothems in the Eastern Mediterranean region and their implication for paleorainfall during interglacial intervals, Geochim. Cosmochim. Ac., 67, 3181–3199, 2003.

Bordon, A., Peyron, O., Lézine, A., Brewer, S., and Fouache, E.: Pollen-inferred Late-Glacial and Holocene climate in southern Balkans (Lake Maliq), Quatern. Int., 200, 19–30, 2009.

Caress, D. and Chayes, D.: MB-SYSTEM Release 5, www.ldgo.columbia.edu/MB-System, last accessed: 21 January 2010, 2005.

Catuneanu, O., Abreu, V., Bhattacharya, J., Blum, M., Dalrymple, R., Eriksson, P., Fielding, C., Fisher, W., Galloway, W., and Gibling, M.: Towards the standardization of sequence stratigraphy, Earth Science Reviews, 92, 1–33, 2009.

Croudace, I., Rindby, A., and Rothwell, G.: ITRAX: description and evaluation of a new multifunction X-ray core scanner, New techniques in sediment core analysis, 267, 51–63, 2006.

D'Agostino, K., Seltzer, G., Baker, P., Fritz, S., and Dunbar, R.: Late-Quaternary lowstands of Lake Titicaca: evidence from high-resolution seismic data, Palaeogeogr. Palaeocl., 179, 97–111, 2002.

Danzeglocke, U., Jöris, O., and Weninger, B.: CalPal-2007online, http://calpal_online.de/, 2008.

Daut, G., Mäusbacher, R., Baade, J., Gleixner, G., Kroemer, E., Mügler, I., Wallner, J., Wang, J., and Zhu, L.: Late Quaternary hydrological changes inferred from lake level fluctuations of Nam Co (Tibetan Plateau, China), Quatern. Int., 218, 86–93, doi:10.1016/j.quaint.2010.01.001, 2010.

De Vivo, B., Rolandi, G., Gans, P., Calvert, A., Bohrson, W., Spera, F., and Belkin, H.: New constraints on the pyroclastic eruptive history of the Campanian volcanic Plain (Italy), Miner. Petrol., 73, 47–65, 2001.

Drysdale, R., Zanchetta, G., Hellstrom, J., Fallick, A., and Zhao, J.: Stalagmite evidence for the onset of the Last Interglacial in southern Europe at 129 ± 1 ka, Geophys. Res. Lett., 32, L24708, doi:10.1029/2005GL024658, 2005.

Stratigraphic analysis of lake level fluctuations in Lake Ohrid

K. Lindhorst et al.

Title Page

Abstract	Introduction
Conclusions	References
Tables	Figures

| ◄◄ | ►► |
| ◄ | ► |

Back | Close

Full Screen / Esc

Printer-friendly Version

Interactive Discussion

Dumurdzanov, N., Serafimovski, T., and Burchfiel, B.: Cenozoic tectonics of Macedonia and its relation to the South Balkan extensional regime, Geosphere, 1, 1–22, 2005.

Genner, M., Knight, M., Haesler, M., and Turner, G.: Establishment and expansion of Lake Malawi rock fish populations after a dramatic Late Pleistocene lake level rise, Mol. Ecol., 19, 170, doi:10.1111/j.1365-294X.2009.04434.x, 2010.

Gilbert, G.: Lake Bonneville, United States Geological Survey, 1890.

Hauffe, T., Albrecht, C., Schreiber, K., Trajanovski, S., and Wilke, T.: gastropods, Biogeosciences Discuss, submitted, 2010.

Hayes, A., Kucera, M., Kallel, N., Sbaffi, L., and Rohling, E.: Glacial Mediterranean sea surface temperatures based on planktonic foraminiferal assemblages, Quaternary Science Reviews, 24, 999-1-016, 2005.

Helland-Hansen, W. and Martinsen, O.: Shoreline trajectories and sequences: description of variable depositional-dip scenarios, J. Sediment. Res. B, 66, 670–688, 1996.

Hoffmann, N., Reicherter, K., Grützner, Ch., Hürtgen, J., Rudersdorf, A., and Viehberg, F. A.: Quaternary evolution of the delta systems and the coast line of Lake Ohrid (FYROM/Albania) revealed by shallow geophysical and drilling data, Biogeosciences Discuss, submitted, 2010.

Hughes, P., Woodward, J., and Gibbard, P.: Quaternary glacial history of the Mediterranean mountains, Prog. Phys. Geog., 30, 334–364, doi:10.1191/0309133306pp481ra, 2006.

Hunt, D. and Tucker, M.: Stranded parasequences and the forced regressive wedge systems tract: deposition during base-level fall, Sediment. Geol., 81, 1–9, 1992.

Johnson, T., Scholz, C., Talbot, M., Kelts, K., Ricketts, R., Ngobi, G., Beuning, K., Ssemmanda, I., and McGill, J.: Late Pleistocene desiccation of Lake Victoria and rapid evolution of cichlid fishes, Science, 273, 1091–1093, doi:10.1126/science.273.5278.1091, 1996.

Keller, J., Ryan, W., Ninkovich, D., and Altherr, R.: Explosive volcanic activity in the Mediterranean over the past 200,000 yr as recorded in deep-sea sediments, Bull. Geol. Soc. Am., 89, 591–604, 1978.

Kraml, M.: Laser-Ar/Ar-Datierungen und distalen marinen Tephren des jung-quartären mediterranen Vulkanismus (Ionisches Meer, M25/4), Ph. D., Albert-Ludwings-Universität Freiburg, Freiburg, 216 pp., 1997.

Lamothe, M., Auclair, M., Hamzaoui, C., and Huot, S.: Towards a prediction of long-term anomalous fading of feldspar IRSL, Radiation measurements, 37, 493–498, 2003.

Magny, M., Peyron, O., Gauthier, E., Rouèche, Y., Bordon, A., Billaud, Y., Chapron, E., Marguet, A., Pétrequin, P., and Vannière, B.: Quantitative reconstruction of climatic variations during

the Bronze and early Iron ages based on pollen and lake-level data in the NW Alps, France, Quatern. Int., 200, 102–110, 2009.

Marino, G., Rohling, E., Sangiorgi, F., Hayes, A., Casford, J., Lotter, A., Kucera, M., and Brinkhuis, H.: Early and middle Holocene in the Aegean Sea: interplay between high and low latitude climate variability, Quaternary Science Reviews, 2009.

Martens, K.: Speciation in ancient lakes, Trends in Ecology & Evolution, 12, 177–182, 1997.

Martrat, B., Grimalt, J., Lopez-Martinez, C., Cacho, I., Sierro, F., Flores, J., Zahn, R., Canals, M., Curtis, J., and Hodell, D.: Abrupt temperature changes in the Western Mediterranean over the past 250,000 years, Science, 306, 1762, 2004.

Matzinger, A., Spirkovski, Z., Patceva, S., and Wuest, A.: Sensitivity of ancient Lake Ohrid to local anthropogenic impacts and global warming, J. Great Lakes Res., 32, 158–179, 2006.

Moernaut, J., Verschuren, D., Charlet, F., Kristen, I., Fagot, M., and Batist, M. D.: The seismic-stratigraphic record of lake-level fluctuations in Lake Challa: Hydrological stability and change in equatorial East Africa over the last 140 kyr, Earth Planet. Sc. Lett., 10, 214–223, doi:10.1016/j.epsl.2009.12.023, 2010.

Paterne, M., Guichard, F., and Labeyrie, J.: Explosive activity of the South Italian volcanoes during the past 80,000 years as determined by marine tephrochronology, J. Volcanol. Geoth. Res., 34, 153–172, 1988.

Peyron, O., Guiot, J., Cheddadi, R., Tarasov, P., Reille, M., de Beaulieu, J., Bottema, S., and Andrieu, V.: Climatic reconstruction in Europe for 18,000 yr BP from pollen data, Quaternary Res., 49, 183–196, 1998.

Pirmez, C., Pratson, L., and Steckler, M.: Clinoform development by advection-diffusion of suspended sediment: Modeling and comparison to natural systems, J. Geophys. Res.-Sol. Ea., 103, 24141–24157, 1998.

Popovska, C. and Bonacci, O.: Basic data on the hydrology of Lakes Ohrid and Prespa, Hydrol. Process., 21, 658–664, 2007.

Posamentier, H., Allen, G., James, D., and Tesson, M.: Forced regressions in a sequence strati-graphic framework: concepts, examples, and exploration significance, AAPG BULLETIN, 76, 1687–1687, 1992.

Preusser, F., Degering, D., Fuchs, M., Hilgers, A., Kadereit, A., Klasen, N., Krbetschek, M., Richter, D., and Spencer, J.: Luminescence dating: Basics, methods and applications, Quaternary Science Journal (Eiszeitalter und Gegenwart), 57, 95–149, 2008.

Schellmann, G., Beerten, K., and Radtke, U.: Electron spin resonance (ESR) dating of Quater-

Title Page

Abstract | Introduction

Conclusions | References

Tables | Figures

◄ | ►

◄ | ►

Back | Close

Full Screen / Esc

Printer-friendly Version

Interactive Discussion

nary materials, Eiszeitalter und Gegenwart 57, 150–178, 2008.

Scholz, C. and Rosendahl, B.: Low lake stands in Lakes Malawi and Tanganyika, East Africa, delineated with multifold seismic data, Science, 240, 1645–1648, 1988.

Spirkovski, Z., Avramovski, O., and Kodzoman, A.: Watershed management in the Lake Ohrid region of Albania and Macedonia, Lakes & reservoirs: research and management, 6, 237–242, 2001.

Stankovic, S.: The Balkan Lake Ohrid and Its Living World, W. Junk, 1960.

Sturmbauer, C., Baric, S., Salzburger, W., Ruber, L., and Verheyen, E.: Lake level fluctuations synchronize genetic divergences of cichlid fishes in African lakes, Mol. Biol. Evol., 18, 144–154, 2001.

Sulpizio, R., Zanchetta, G., Paterne, M., and Siani, G.: A review of tephrostratigraphy in central and southern Italy during the last 65 ka, Il Quaternario, 16, 91–108, 2003.

Sulpizio, R., Zanchetta, G., D'orazio, M., Vogel, H., and Wagner, B.: Tephrostratigraphy and tephrochronology of the lakes Ohrid and Prespa, Balkans, Biogeosciences Discuss, submitted, 2010.

Susnik, S., Knizhin, I., Snoj, A., and Weiss, S.: Genetic and morphological characterization of a Lake, J. Fish Biol., 68, 2–23, 2006.

Tzedakis, P., Frogley, M., and Heaton, T.: Last Interglacial conditions in southern Europe: evidence from Ioannina, northwest Greece, Global Planet. Change, 36, 157–170, 2003.

Vogel, H., Wagner, B., Zanchetta, G., Sulpizio, R., and Rosén, P.: A paleoclimate record with tephrochronological age control for the last glacial-interglacial cylce from Lake Ohrid, Albania and Macedonia, J. Paleolimnol., doi:10.1007/s10933-009-9404-x, 2010a.

Vogel, H., Zanchetta, G., Sulpizio, R., Wagner, B., and Nowaczyk, N.: A tephrostratigraphic record for the last glacial–interglacial cycle from Lake Ohrid, Albania and Macedonia., J. Quaternary Sci., 25, 320–338, 2010b.

Wagner, B., Reicherter, K., Daut, G., Wessels, M., Matzinger, A., Schwalb, A., Spirkovski, Z., and Sanxhaku, M.: The potential of Lake Ohrid for long-term palaeoenvironmental reconstructions, Palaeogeogr. Palaeocl., 259, 341–356, 2008a.

Wagner, B., Sulpizio, R., Zanchetta, G., Wulf, S., Wessels, M., Daut, G., and Nowaczyk, N.: The last 40 ka tephrostratigraphic record of Lake Ohrid, Albania and Macedonia: a very distal archive for ash dispersal from Italian volcanoes, J. Volcanol. Geoth. Res., 177, 71–80, 2008b.

Title Page

Abstract | Introduction

Conclusions | References

Tables | Figures

|◄ | ►|

◄ | ►

Back | Close

Full Screen / Esc

Printer-friendly Version

Interactive Discussion

Wagner, B., Lotter, A., Nowaczyk, N., Reed, J., Schwalb, A., Sulpizio, R., Valsecchi, V., Wessels, M., and Zanchetta, G.: A 40,000-year record of environmental change from ancient Lake Ohrid (Albania and Macedonia), J. Paleolimnol., 41, 407–430, 2009.

Wallinga, J., Bos, A., Dorenbos, P., Murray, A., and Schokker, J.: A test case for anomalous fading correction in IRSL dating, Quat. Geochronol., 2, 216–221, 2007.

Watzin, M. C., Puka, V., and Naumoski, T.: Lake Ohrid and its Watershed, State of the Environment Report, Lake Ohrid Conservation Project., 134 pp, 2002.

Wessel, P. and Smith, W.: Free software helps map and display data, Eos Trans. AGU, 72, 445–446, 1991.

Zanchetta, G., Sulpizio, R., Giaccio, B., Siani, G., Paterne, M., Wulf, S., and D'Orazio, M.: The Y-3 tephra: A Last Glacial stratigraphic marker for the central Mediterranean basin, J. Volcanol. Geoth. Res., 177, 145–154, 2008.

Stratigraphic analysis of lake level fluctuations in Lake Ohrid

K. Lindhorst et al.

Table 1. Radiocarbon ages (yr BP) and calendar ages (cal. Yr BP) inferred using CalPal-2007 online (Danzeglocke et al., 2008) of plant macrofossils from cores Co1200 and Co1201.

Sample ID	Core ID	Depth (cm)	^{14}C age (yr BP)	Calendar age (cal. yr BP)
KIA37138	Co1200	6	1954 AD	1954 AD
KIA37139	Co1200	13	21610 ± 185	25815 ± 522
KIA37140	Co1201	15	5010 ± 35	5773 ± 82
KIA37141	Co1201	18	15810 ± 155	19030 ± 244

Table 2. Dating results and radioactivity data. Ages from core Co1201 were derived by IRSL dating, sample K-5764 from core Co1200 was ESR[1] dated.

Lab. Code	Sample ID	Water content (weight-%)[2]	Burial depth (m)	U (ppm)[3]	Th (ppm)	K (%)	De (Gy)	D_0 (Gy ka^{-1})	Age (ka)	IRSL-Age Fading corrected (ka)
C-L2573	Co1201-5 I (372–409 cm)	30.3 ± 4.5	17.75	4.11 ± 0.14	15.75 ± 0.72	2.45 ± 0.05	479.6 ± 33.0	4.0 ± 0.2	119 ± 10	157 ± 21
C-L2574	Co1201-5 I (409–456 cm)	29.9 ± 4.5	17.95	4.19 ± 0.14	16.00 ± 0.74	2.47 ± 0.05	558.0 ± 31.8	4.1 ± 0.3	137 ± 127	181 ± 24
C-L2575	Co1201-5 III (556–604 cm)	29.2 ± 4.4	19.50	3.76 ± 0.13	14.86 ± 0.68	2.45 ± 0.05	372.3 ± 24.6	4.0 ± 0.2	93.4 ± 8.1	123 ± 16
C-L2576	Co1201-5 III (604–656 cm)	30.9 ± 4.6	20.00	4.04 ± 0.14	15.67 ± 0.72	2.50 ± 0.05	438.1 ± 40.2	4.0 ± 0.3	109 ± 12	143 ± 21
K-5764	Co1200-6 III (200–232 cm)	35-50		0.41 ± 0.04	0.33 ± 0.03	0.06 ± 0.01	16.40 ± 1.23		130 ± 28	

[1] The dose rates and ESR-ages were calculated for different water contents and different thicknesses of an overlying sediment unit and water column, as the depositional history was complex. The age estimate is the average from the maximum and minimum ages resulting from dose rate modelling.
[2] Water content is the in-situ water content with 15% uncertainty.
[3] Internal U-content: 0.07 ± 0.01 ppm.

Title Page

Abstract | Introduction

Conclusions | References

Tables | Figures

|◄ | ►|

◄ | ►

Back | Close

Full Screen / Esc

Printer-friendly Version

Interactive Discussion

Table 3. Relationship between morphological, seismic (multichannel and sediment echosounder) and lithological data of Ohrid Bay. LGM=Last Glacial Maximum, MIS=Marine Isotop Stage.

Morphology	stratigraphy		cores	system tracts	age	lake level	base level	shoreline trajectory
	seismic units	Litho-facies						
step 1								
upper terrace	H	I	Co1200	HST 9	Holocene	modern		transgression
	G	II	Co1200	HST 9	LGM	modern		transgression
	F	III	Co1200	FRST 8	MIS 5	stage 3	~35 m	minor regression
step 2	outcrop F	III	Co1200	FRST 8	MIS 5	stage 3	~35 m	minor regression
lower terrace	H	I	Co1201	HST 9	Holocene	modern		transgression
	G	II	Co1201	HST 9	LGM	modern		transgression
	E_2	-	-	HST 7	late MIS 6/ MIS 5	stage 2	~25 m	transgression
	E_1	IV	Co1201	FRST 6	MIS 6	stage 1	~55 m	continuous regression
step 3	outcrop E	IV	Co1201	FRST 6	MIS 6	stage 1	~55 m	continuous regression
deep central basin								
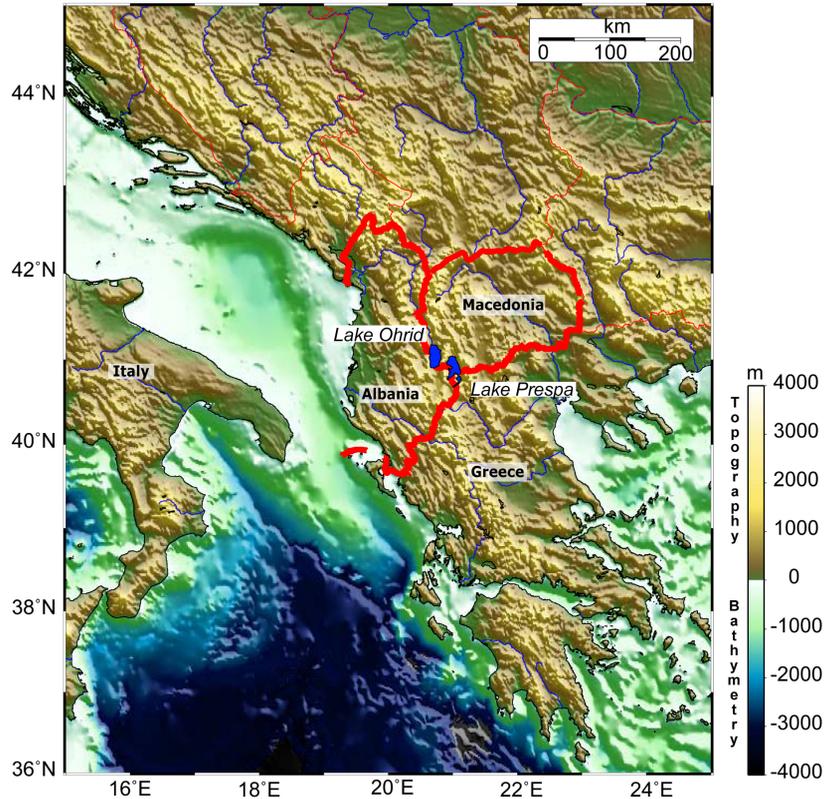
Fig. 1. Map of southern Europe with Lake Ohrid and its sister Lake Prespa situated on the Balkan Peninsula.
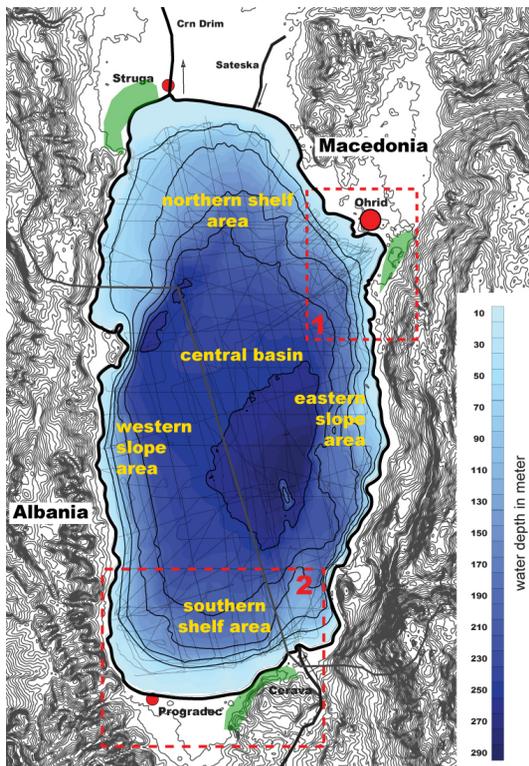
Fig. 2. Bathymetric and topographic map of ancient Lake Ohrid and surrounding area. The lake can be divided into five morphological sections: Ohrid Bay, southern and northern shelf area, western and eastern slope area, and central basin. Three rivers: Crn Drim, Sateska, and Cerava are marked with an arrow indicating the direction of flow. Red dashed line indicates two major study areas: 1: Ohrid Bay, 2: southern area. Gray line is the boundary between Macedonia and Albania. Light green are spring areas and light gray lines mark seismic surveys since 2004.
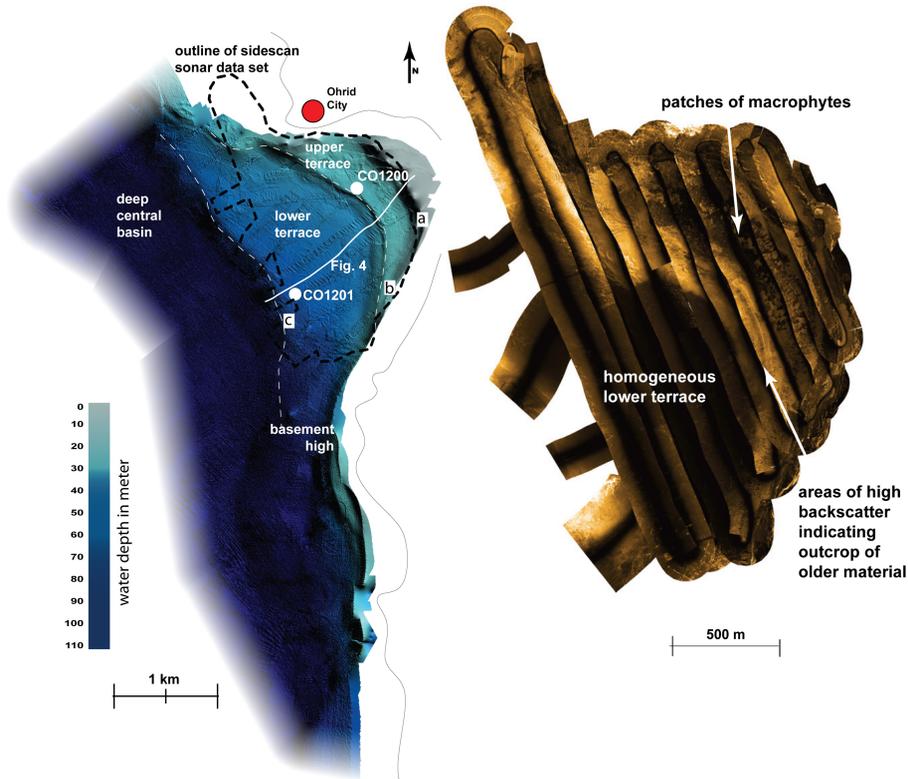
Fig. 3. Bathymetric map of Ohrid Bay (left) with major morphological features such as upper and lower terrace, deep central basin, three morphological steps (a, b, c at water depth 15 m, 33 m, and 55 m, respectively). Sediment cores (Co1200, Co1201) are marked. Sidescan sonar mosaic (right) images the upper portion of Ohrid Bay. The outline of the sidescan sonar mosaic is shown as dashed line. Note the different scales for each map. An outline of the sidescan mosaic is marked in the bathymetric map. See Fig. 2 for location.

Fig. 4. Sediment echo sounder profile across Ohrid Bay (see map inlet for location) running in a east-west direction over a distance of 2 km. **(A)** uninterpreted section with projection of sediment cores **(B)** line drawing and interpretation of the section. The profile shows the internal structure of the upper and lower terraces. Seismic units E_1, E_2 F, G, H and System tracts 6, 7, 8, 9, tephra layer most likely assigned to (CI)/Y5 and areas with mass wasting deposits as evidenced by a hummocky topography are labeled. Morphological section with slope angles is indicated at the bottom.

Title Page

Abstract | Introduction

Conclusions | References

Tables | Figures

◄◄ | ►►

◄ | ►

Back | Close

Full Screen / Esc

Printer-friendly Version

Interactive Discussion

Title Page

Abstract | Introduction

Conclusions | References

Tables | Figures

◄ | ►|

◄ | ►

Back | Close

Full Screen / Esc

Printer-friendly Version

Interactive Discussion
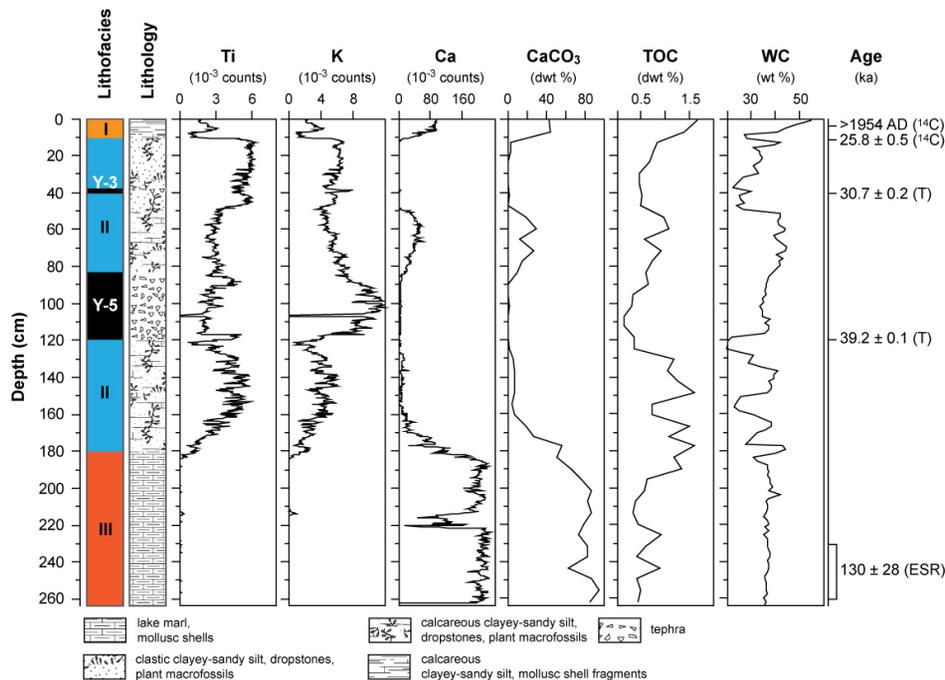
Fig. 5. Lithofacies, lithology, Ti-, K-, Ca- intensities, CaCO$_3$, total organic carbon (TOC) dry weight percentages, water content (WC), and age control points of core Co1200. ^{14}C=calibrated radiocarbon age, T=tephra age, ESR=electron spin resonance age. Location of core is shown on Fig. 3.
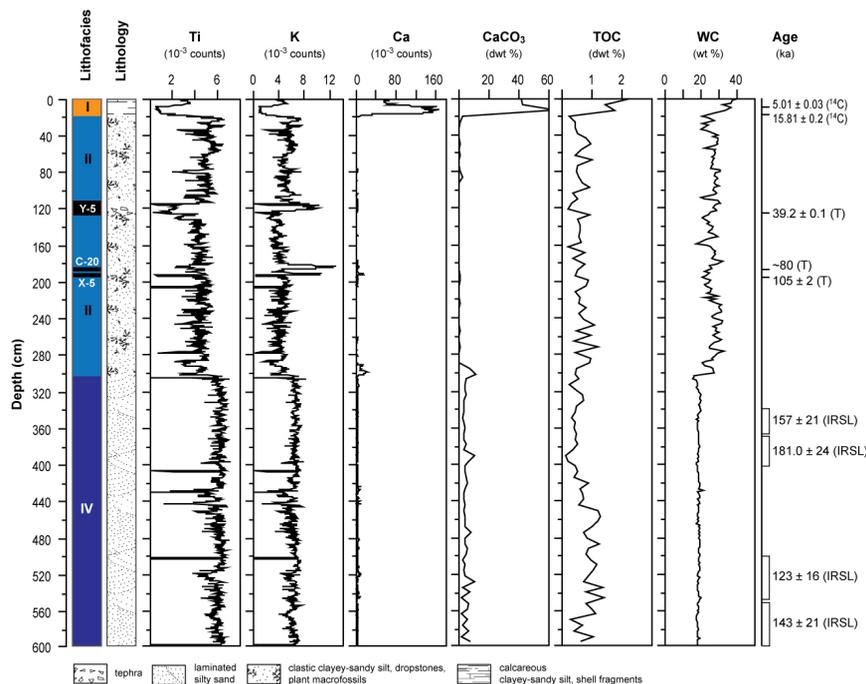
Fig. 6. Lithofacies, lithology, Ti-, K-, Ca- intensities, $CaCO_3$, total organic carbon (TOC) dry weight percentages, water content (WC), and age control points of core Co1201. [14]C=calibrated radiocarbon age, T=tephra age, IRSL=infrared stimulated luminescence age. Location of core is shown on Fig. 3.
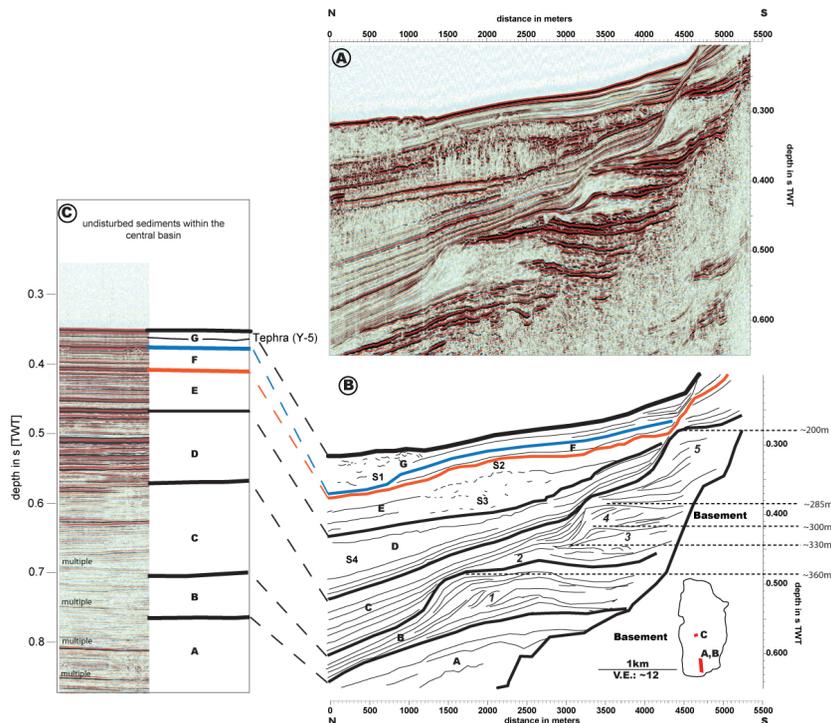
Fig. 7. Multichannel seismic cross section of sedimentary structures within the southern area running in a north-south direction over a distance of 5.5 km. **(A)** uninterpreted and **(B)** interpreted section. Interpretation of the seismic section shows that Lake Ohrid has a complex sedimentary evolution with a stepwise rose of lake level since its existence as water filled body as suggested by five major clinoform structures (1–5). Within younger sequences several mass wasting deposits have been found indicating that sliding events are common in the southern area. A correlation of prominent reflections that bound major seismic units (A–G) with well stratified sediments in the central basin of Lake Ohrid is shown in **(C)**.
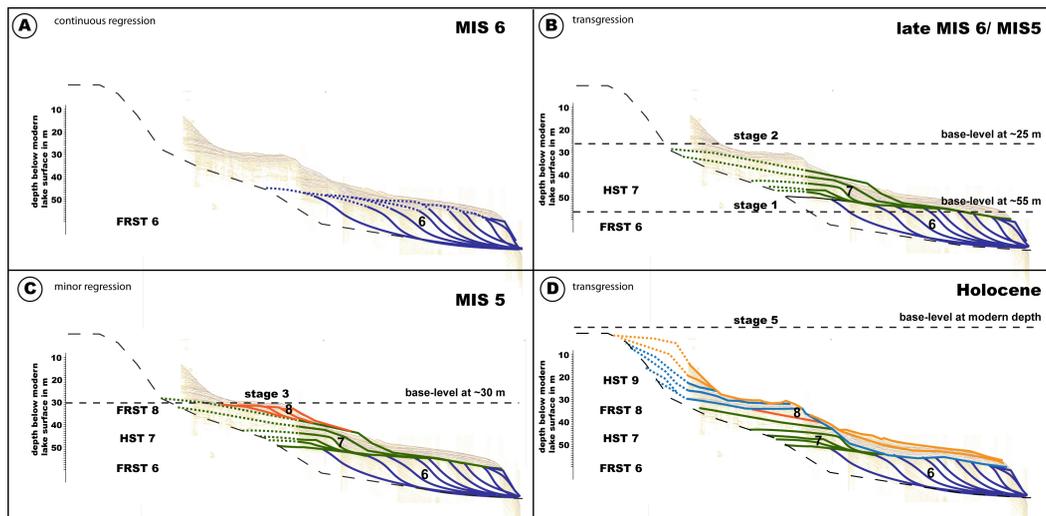
Fig. 8. A conceptual model that illustrates the sedimentary evolution of terraces in Ohrid Bay since MIS 6 (penultimate glacial period). FRST=Forced Regression System Tract, HST=Highstand System Tract, MIS=Marine Isotope Stage. Because clinoforms within the southern area are relatively older than those in Ohrid Bay this model starts with FRST 6. After a continuous regression during MIS 6 with subsequent formation of FRST 6 **(A)** the lake level rose of about 30 m as indicated by HST 7 **(B)**. This period is followed by a falling relative lake level evidenced by FRST 8 **(C)**. After a lowstand with an exposure of the upper terrace and subsequent erosion of HST 7 and FRST 8 the lake level rose to modern water depth with deposition of sediments assigned to lithofacies II and I **(D)**.
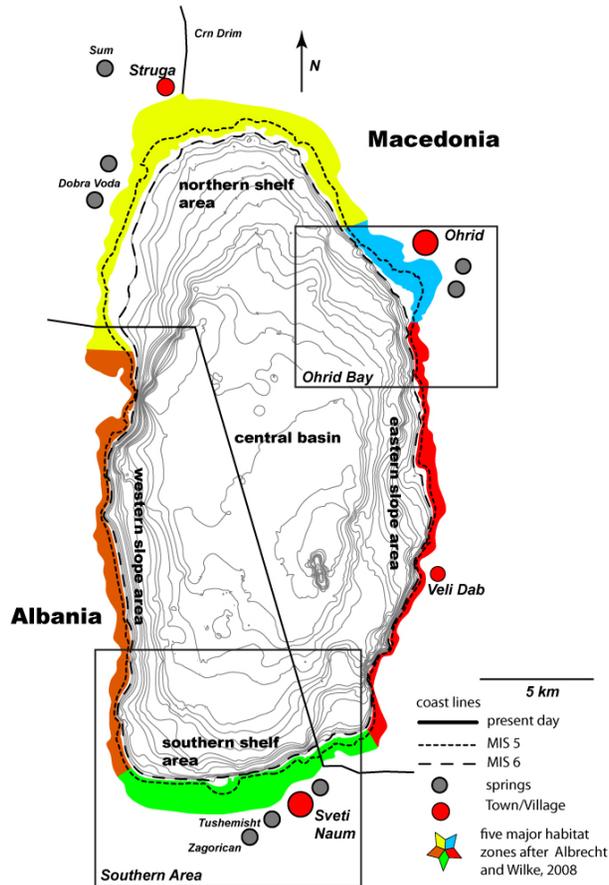
Fig. 9. Map of Lake Ohrid with major habitat zones (Albrecht and Wilke, 2008). Ancient coastlines as inferred from geophysical and sedimentological data in Ohrid Bay are marked. Spring areas around Sveti Naum (Zagorican, Tushemisht), Ohrid Bay, and west of Struga (Dobra Voda, Sum) are labeled.